Available online at www.elixirpublishers.com (Elixir International Journal)

Applied Mathematics

Elixir Appl. Math. 76 (2014) 28367-28380

ISSN: 2229-712X

Two phase boundary layer flow and heat transfer using non-uniform grid

P. K. Tripathy[1], A.Misra[2], S. K. Mishra[2] and J. Prakash[3,*]

[1]Department of Mathematics and Science, U.C.P. Engg. School, Berhampur, Ganjam (Odisha), India.

[2]Department of Mathematics, Centurion University of Technology and Management,Paralakhemundi,Gajapati-761211,Odisha, India.

[3]Department of Mathematics, Faculty of Science, University of Botswana, Private Bag 0022, Gaborone, Botswana.

ARTICLE INFO

Article history:
Received: 30 September 2014;
Received in revised form:
27 October 2014;
Accepted: 6 November 2014;

Keywords
Volume Fraction,
Suspended Particulate Matter,
Two Phase Flow,
Boundary Layer Characteristics,
Slip Velocity, Heat Transfer.

ABSTRACT

The knowledge of the structure of the boundary layer gives an idea to understand the capabilities of the atmosphere to dispose of pollutants. Finite difference technique with non-uniform grid is used to investigate the effect of various flow parameters on skin friction , heat transfer and other characteristics of two phase thermal boundary layer flow on a flat plate. Heat is diffused away from the heated surface for smaller values of Prandtl number P_r more rapidly than that of higher values of P_r. The particle density on the plate goes on increasing and attains a finite value of 3.5 at a far down stream station. The presence of coarser particles with high material density have an effect of increase in magnitude of particle velocity and particle phase density whereas to reduce the particle temperature. The increase in Prandtl number P_r is to increase the magnitude of carrier fluid velocity, particle velocity, particle phase density, coefficient of skin friction and Nusselt number where as to decrease the displacement thickness.

Introduction

The flow of fluid with suspended particulate matter (SPM) has received the attention of many workers due to its possible industrial applications like sedimentation, pipe flows, fluidized beds, gas – purification and transport process. The conservation equations for two phase flow by considering a distribution of spherical solid particles having the same radius are found in the references [1 – 8 , 12, 13].The effect of volume fraction and diffusion of SPM have been studied in different situations which appears in the literature [9 – 11, 15 – 19]. The boundary layer assumptions made by Chiu [19] are incorrect as the conservation of the particle momentum equation in the normal direction is neglected. Marble [12] analysis is not applicable for the entire length of the plate. Ghosh [4] has studied the laminar boundary layer flow on a flat plate employing momentum integral method and their solution is valid towards a far down stream portions of the plate. Prabha and Jain [5] have employed the finite difference technique to study the laminar boundary layer flow over a flat plate, but have not considered the momentum equation in the normal direction. Singleton [2] has derived the results in small slip and large slip regions in the compressive boundary layer flow over a flat plate by taking momentum equation in normal direction. Chamakha [7, 8] has considered the channel flow by including the finite volume fraction and electrification of the particles. Mishra & Tripathy [15, 16] have studied the flow situation over a flat plate, where effect of volume fraction on the flow has not been studied.

In the present problem, the effect of volume fraction on skin friction, heat transfer and other boundary layer characteristics have been studied by employing finite difference technique using non – uniform grid. In this study, the momentum equation for particulate phase in normal direction, heat due to conduction and viscous dissipation in the energy equation of the particle phase have been considered for better understanding of the boundary layer characteristics. Here particles are allowed to diffuse through the career fluid i.e. the random motion of the particles are taken into account because of the small size of the particles which can be done by applying the kinetic theory of gases. Hence the motion of the particles across the streamline is due to the concentration and pressure diffusion. Therefore, the density of the mixture of career fluid and particles is given by

$$\boldsymbol{\rho_m = \rho_p + \rho\left(1 - \frac{\rho_p}{\rho_s}\right)}. \qquad (1)$$

The factor $\left(\mathbf{1} - \frac{\rho_p}{\rho_s}\right)$ accounts for the volume occupied by the particles in the career fluid. Then we can write

Tele:
E-mail addresses: prakashj@mopipi.ub.bw

$$\rho_m\overrightarrow{q_m} = \rho_p\overrightarrow{q_p} + \rho\left(1-\frac{\rho_p}{\rho_s}\right)\overrightarrow{q}. \qquad (2)$$

The career fluid flow is of boundary layer type and there is a large concentration gradient in Y – direction. So the particles diffuse slowly in Y – direction due to their large size as compared to fluid molecules. The continuity equation of the mixture is given by

$$\frac{\partial(\rho_m u_m)}{\partial x} + \frac{\partial(\rho_m v_m)}{\partial \eta} = 0 \qquad (3)$$

From Equations (1) and (3), we get

$$\frac{\partial(\rho_p u_p)}{\partial x} + \frac{\partial(\rho_p v_p)}{\partial y} + \rho\left(1-\frac{\rho_p}{\rho_s}\right)\left(\frac{\partial u}{\partial x} + \frac{\partial v}{\partial y}\right) - u\frac{\rho}{\rho_s}\frac{\partial \rho_p}{\partial x} - v\frac{\rho}{\rho_s}\frac{\partial \rho_p}{\partial y} = 0 \qquad (4)$$

The last two terms in the Equation (4) can be neglected and the third term is zero. So, the continuity equation for the particle phase is given by

$$\frac{\partial(\rho_p u_p)}{\partial x} + \frac{\partial(\rho_p v_p)}{\partial y} = 0 \qquad (5)$$

To calculate the particle concentration, we need in general two dynamical equations for u_p and v_p. Also, it is possible to treat the particle cloud as a fluid and to calculate the particle concentration by making use of the diffusion equation. Since the flow is of boundary layer type, the relevant equation after neglecting the lower order terms is then,

$$u_p\frac{\partial \rho_p}{\partial x} + v_p\frac{\partial \rho_p}{\partial y} = D_p\frac{\partial^2 \rho_p}{\partial y^2} \qquad (6)$$

D_p can be taken as a constant as the temperature variation in the flow is assumed to be small i.e. $D_p \approx \nu_p$ and often quite small in comparison with ν.

Mathematical Formulation:

Considered the steady flow of a viscous incompressible fluid with uniformly distributed suspended particles past a thin semi-infinite flat plate at a constant temperature T_w, placed along the direction of a uniform stream of velocity *U* and temperature T_∞.Let the plate lie in x-z plane and the flow of free stream to be in the x- direction. Refer to the physical model given below:

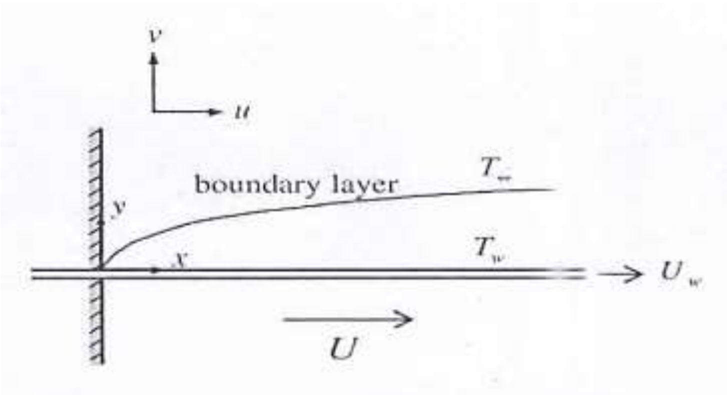

Fig. 1. Physical model and coordinate system.

Otterman [3] has shown that the standard boundary layer approximations are valid for the fluid phase provided that the density of the particulate phase is of the same order as that of the fluid. Further it has been shown that the boundary layer approximation of the momentum equations for the particle phase is not necessary and that the particle momentum equations in the transverse direction cannot be neglected. Under the above circumstances the y – component of the momentum equation of the fluid phase is dropped whereas the y – component of momentum equation of the particle phase is retained.

Introducing the non- dimensional variables

$$x^* = \frac{x}{L},\ \eta = \frac{y}{L}\sqrt{Re},\quad u^* = \frac{u}{U},\ v^* = \frac{v}{U}\sqrt{Re},\quad u_p^* = \frac{u_p}{U},\ v_p^* = \frac{v_p}{U}\sqrt{Re},$$
$$T^* = \frac{T-T_\infty}{T_w-T_\infty},\ T_p{}^* = \frac{T_p-T_\infty}{T_w-T_\infty},\quad \rho_p^* = \frac{\rho_p}{\rho_{p_0}} \qquad (7)$$

The governing boundary layer equations of the flow field as discussed in the references [1-8, 17], after dropping stars are given by

$$\frac{\partial u}{\partial x} + \frac{\partial v}{\partial \eta} = 0 \tag{8}$$

$$u_p \frac{\partial \rho_p}{\partial x} + v_p \frac{\partial \rho_p}{\partial \eta} = \epsilon \frac{\partial^2 u_p}{\partial \eta^2} \tag{9}$$

$$u \frac{\partial u}{\partial x} + v \frac{\partial u}{\partial \eta} = \frac{\partial^2 u}{\partial \eta^2} - \alpha \frac{\varphi}{1-\varphi} \frac{F\,L}{U} \rho_p (u - u_p) \tag{10}$$

$$u_p \frac{\partial u_p}{\partial x} + v_p \frac{\partial u_p}{\partial \eta} = \epsilon \frac{\partial^2 u_p}{\partial \eta^2} + \frac{F\,L}{U}(u - u_p) \tag{11}$$

$$u_p \frac{\partial v_p}{\partial x} + v_p \frac{\partial v_p}{\partial \eta} = \epsilon \frac{\partial^2 v_p}{\partial \eta^2} + \frac{F\,L}{U}(v - v_p) \tag{12}$$

$$u \frac{\partial T}{\partial x} + v \frac{\partial T}{\partial \eta} = \frac{1}{Pr} \frac{\partial^2 T}{\partial \eta^2} + Ec \left(\frac{\partial u}{\partial \eta}\right)^2 + \frac{2\,\alpha}{3\,Pr} \frac{\varphi}{1-\varphi} \frac{F\,L}{U} \rho_p (T_p - T) \tag{13}$$

$$u_p \frac{\partial T_p}{\partial x} + v_p \frac{\partial T_p}{\partial \eta} = \frac{F\,L}{U} (T - T_p) + \frac{\epsilon}{Pr} \frac{\partial^2 T_p}{\partial \eta^2} + \epsilon . Ec \left[\left(\frac{\partial u_p}{\partial \eta}\right)^2 + u_p \frac{\partial^2 u_p}{\partial \eta^2}\right] \tag{14}$$

subject to the boundary conditions

$$\eta = 0 \; : u = 0, \quad v = 0, u_p = u_{pw}(x), \quad v_p = 0, \; \rho_p = \rho_{pw}(x), \quad T = 1, \quad T_p = T_{pw}(x) \tag{15}$$

$$\eta = \infty \; : u = u_p = \rho_p = 1, \; v_p = 0, \quad T = 0, \quad T_p = 0 \tag{16}$$

Reducing the Equations (8) - (14) into difference equations, we get

$$v_j^{n+1} = v_{j-1}^{n+1} - \frac{1}{2} \frac{\Delta y}{\Delta x} \left[\left(1.5 \; u_j^{n+1} - 2\, u_j^n + 0.5\, u_j^{n-1}\right) + \left(1.5 \; u_{j-1}^{n+1} - 2\, u_{j-1}^n + 0.5\, u_{j-1}^{n-1}\right)\right] \tag{17}$$

$$a_j u_{j-1}^{n+1} + b_j u_j^{n+1} + c_j u_{j+1}^{n+1} = d_j \tag{18}$$

$$a_j^* {u_p}_{j-1}^{n+1} + b_j^* {u_p}_j^{n+1} + c_j^* {u_p}_{j+1}^{n+1} = d_j^* \tag{19}$$

$$a_j^{**} {v_p}_{j-1}^{n+1} + b_j^{**} {v_p}_j^{n+1} + c_j^{**} {v_p}_{j+1}^{n+1} = d_j^{**} \tag{20}$$

$$a_j^+ T_{j-1}^{n+1} + b_j^+ T_j^{n+1} + c_j^+ T_{j+1}^{n+1} = d_j^+ \tag{21}$$

$$a_j^{++} {T_p}_{j-1}^{n+1} + b_j^{++} {T_p}_j^{n+1} + c_j^{++} {T_p}_{j+1}^{n+1} = d_j^{++} \tag{22}$$

$$a_j^{\blacksquare} {\rho_p}_{j-1}^{n+1} + b_j^{\blacksquare} {\rho_p}_j^{n+1} + c_j^{\blacksquare} {\rho_p}_{j+1}^{n+1} = d_j^{\blacksquare} \tag{23}$$

by replacing

$$\frac{\partial W}{\partial x} = \frac{1.5\, W_j^{n+1} - 2 W_j^n + 0.5\, W_j^{n-1}}{\Delta x} + O(\Delta x^2) \tag{24}$$

$$\frac{\partial W}{\partial y} = \frac{W_{j+1}^{n+1} - (1 - r_y^2) W_j^{n+1} - r_y^2\, W_{j-1}^{n+1}}{r_y\,(r_y + 1)\, \Delta y_j} + O(\Delta y^2) \tag{25}$$

$$\frac{\partial^2 W}{\partial y^2} = 2\, \frac{W_{j+1}^{n+1} - (1 + r_y) W_j^{n+1} + r_y\, W_{j-1}^{n+1}}{r_y\,(r_y + 1)\, \Delta y_j^2} + O(\Delta y^2) \tag{26}$$

$$W_j^{n+1} = 2\, W_j^n - W_j^{n-1} + O(\Delta x^2) \tag{27}$$

and $y_{j+1} - y_j = r_y \left(y_j - y_{j-1}\right) = r_y \Delta y_j$ (28)

Here a general three point representation of $\frac{\partial W}{\partial y}$ on a non – uniform grid that produces the smallest truncation error is used.

where

$$a_j = \frac{1}{\Delta x} \left[- p r_y - q\right]$$

$$b_j = \frac{1}{\Delta x} \left[1.5 \; \left(2\, u_j^n - u_j^{n-1}\right) + p \left(r_y - \frac{1}{r_y}\right) + q \left(1 + \frac{1}{r_y}\right) + \frac{\varphi}{1-\varphi} \frac{F\,L}{U} \alpha \Delta x \left(2\, {\rho_p}_j^n - {\rho_p}_j^{n-1}\right)\right]$$

$$c_j = \frac{1}{\Delta x} \left[\frac{1}{r_y}(p - q)\right]$$

$$d_j = \frac{1}{\Delta x}\left[\left(2\, u_j^n - u_j^{n-1}\right)\left(2\, u_j^n - 0.5\, u_j^{n-1}\right) - \frac{\varphi}{1-\varphi} \frac{FL}{U} \alpha \Delta x \left(2\, {\rho_p}_j^n - {\rho_p}_j^{n-1}\right)\left(- 2\, {u_p}_j^n + {u_p}_j^{n-1}\right)\right]$$

$$a_j^{*} = \frac{1}{\Delta x}\left[-pr_y - \epsilon q\right]$$

$$b_j^{*} = \frac{1}{\Delta x}\left[1.5\ \left(2\,{u_p}_j^{n} - {u_p}_j^{n-1}\right) + p\left(r_y - \frac{1}{r_y}\right) + \epsilon q\left(1 + \frac{1}{r_y}\right) + \frac{FL}{U}\,\Delta x\right]$$

$$c_j^{*} = \frac{1}{\Delta x}\left[\frac{1}{r_y}(p - \epsilon q)\right]$$

$$d_j^{*} = \frac{1}{\Delta x}\left[\left(2\,{u_p}_j^{n} - {u_p}_j^{n-1}\right)\left(2\,{u_p}_j^{n} - 0.5\,{u_p}_j^{n-1}\right) + \frac{FL}{U}\,\Delta x\,u_j^{n+1}\right]$$

$$a_j^{**} = \frac{1}{\Delta x}\left[-pr_y - \epsilon q\right]$$

$$b_j^{**} = \frac{1}{\Delta x}\left[1.5\ {u_p}_j^{n+1} + p\left(r_y - \frac{1}{r_y}\right) + \epsilon q\left(1 + \frac{1}{r_y}\right) + \frac{FL}{U}\,\Delta x\right]$$

$$c_j^{**} = \frac{1}{\Delta x}\left[\frac{1}{r_y}(p - \epsilon q)\right]$$

$$d_j^{**} = \frac{1}{\Delta x}\left[{u_p}_j^{n+1}\left(2\,{v_p}_j^{n} - 0.5\,{v_p}_j^{n-1}\right) + \frac{FL}{U}\,\Delta x\,v_j^{n+1}\right]$$

$$a_j^{+} = \frac{1}{\Delta x}\left[-q\left(0.5\,r_y\,\Delta y\,v_j^{n+1} + \frac{1}{Pr}\right)\right]$$

$$b_j^{+} = \frac{1}{\Delta x}\left[1.5\,u_j^{n+1} + 0.5\,q\,\Delta y\,v_j^{n+1}\left(r_y - \frac{1}{r_y}\right) + \frac{q\,(1 + r_y)}{Pr.r_y} + \frac{2\alpha}{3\,Pr}\ \frac{\varphi}{1-\varphi}\ \frac{FL}{U}\,\Delta x\,{\rho_p}_j^{n+1}\right]$$

$$c_j^{+} = \frac{1}{\Delta x}\left[\frac{q}{r_y}\left(0.5\,\Delta y\,v_j^{n+1} - \frac{1}{Pr}\right)\right]$$

$$d_j^{+} = \frac{1}{\Delta x}\left[\frac{2\alpha}{3\,Pr}\ \frac{\varphi}{1-\varphi}\ \frac{FL}{U}\ {\rho_p}_j^{n+1}\left(2\,{T_p}_j^{n} - {T_p}_j^{n-1}\right)\Delta x + \Delta x.Ec\left(\frac{u_{j+1}^{n+1} - u_j^{n+1}}{\Delta y}\right)^2 + u_j^{n+1}\left(2\,T_j^{n} - 0.5\,T_j^{n-1}\right)\right]$$

$$a_j^{++} = \frac{1}{\Delta x}\left[-q\left(0.5\,r_y\,\Delta y\,{v_p}_j^{n+1} + \frac{\epsilon}{Pr}\right)\right]$$

$$b_j^{++} = \frac{1}{\Delta x}\left[1.5\,{u_p}_j^{n+1} + 0.5\,q\,\Delta y\,{v_p}_j^{n+1}\left(r_y - \frac{1}{r_y}\right) + \frac{\epsilon\,q\,(1 + r_y)}{Pr.r_y} + \frac{FL}{U}\,\Delta x\right]$$

$$c_j^{++} = \frac{1}{\Delta x}\left[\frac{q}{r_y}\left(0.5\Delta y.{v_p}_j^{n+1} - \frac{\epsilon}{Pr}\right)\right]$$

$$d_j^{++} = \frac{1}{\Delta x}\left[\begin{array}{c} {u_p}_j^{n+1}\left(2\,{T_p}_j^{n} - 0.5\,{T_p}_j^{n-1}\right) + \frac{FL}{U}\ T_j^{n+1}\Delta x \\ +\epsilon.Ec.\Delta x\left\{\left(\frac{{u_p}_{j+1}^{n+1} - {u_p}_j^{n+1}}{\Delta y}\right)^2 + {u_p}_j^{n+1}\left(\frac{{u_p}_{j-1}^{n+1} - \left(1 + \frac{1}{r_y}\right){u_p}_j^{n+1} + \frac{1}{r_y}\,{u_p}_{j+1}^{n+1}}{(1 + r_y)\ \Delta y^2}\right)\right\}\end{array}\right]$$

$$a_j^{\blacksquare} = -{v_p}_j^{n+1} r_y^2\,\Delta y - 2\epsilon\,r_y$$

$$b_j^{\blacksquare} = \frac{1.5\,p^{\blacksquare}\,{u_p}_j^{n+1}}{\Delta x} - {v_p}_j^{n+1}\left(1 - r_y\right)^2\Delta y + 2\epsilon\left(1 + r_y\right)$$

$$c_j^{\blacksquare} = {v_p}_j^{n+1}\Delta y - 2\epsilon \;;\quad d_j^{\blacksquare} = p^{\blacksquare}\,{u_p}_j^{n+1}\,\frac{2{\rho_p}_j^{n} - 0.5\,{\rho_p}_j^{n-1}}{\Delta x} \;;\quad p = \left(2\,v_j^{n} - v_j^{n-1}\right)\frac{\Delta x}{(1 + r_y)\Delta y} \;;$$

$$q = \frac{2\,\Delta x}{(1 + r_y)\,\Delta y^2} \;;\quad p^{\blacksquare} = r_y\left(1 + r_y\right)\Delta y^2$$

Here the Eqs. (18) to (23) are not applicable at $j = 1$ or $j = jmax$ because of the boundary conditions (15) and (16).

Therefore, $a_2 = 0$ as $u_1 = 0$ at $j = 2$

$d_j = d_j - c_j u_e$ at $j = j_{max} - 1$

$$d_2^* = d_2^* - a_2^* v_{pw} \qquad \text{at } j = 2$$

$$d_j^* = d_j^* - c_j^* u_e \qquad \text{at } j = j_{max} - 1$$

$$a_2^{**} = 0 \qquad \text{at } j = 2$$

$$c_j^{**} = 0 \qquad \text{at } j = j_{max} - 1$$

$$d_2^+ = d_2^+ - a_2^+ \qquad \text{at } j = 2$$

$$c_j^+ = 0 \qquad \text{at } j = j_{max} - 1$$

$$d_2^{++} = d_2^{++} - a_2^{++} T_{pw} \qquad \text{at } j = 2$$

$$c_j^{++} = 0 \qquad \text{at } j = j_{max} - 1$$

$$d_2^{\blacksquare} = d_2^{\blacksquare} - a_2^{\blacksquare} \rho_{pw} \qquad \text{at } j = 2$$

$$d_j^{\blacksquare} = d_j^{\blacksquare} - c_j^{\blacksquare} \qquad \text{at } j = j_{max} - 1$$

As no slip condition which is not satisfied by the particles, so u_{pw}, ρ_{pw} and T_{pw} are calculated separately on the plate at $\eta = 0$. As u_{pw} , ρ_{pw} and T_{pw} are functions of x only, so from equations (11), (9) and (14) we obtain

$$\frac{\partial u_{pw}}{\partial x} = -\frac{FL}{U} \tag{29}$$

$$\frac{\partial}{\partial x}\left(\rho_{pw} u_{pw}\right) + \frac{\partial}{\partial y}\left(\rho_p v_p\right) = 0 \;\Rightarrow\; u_{pw}\frac{\partial \rho_{pw}}{\partial x} - \rho_{pw}\frac{FL}{U} = 0 \quad \text{(by using Eq. (29))} \tag{30}$$

$$u_{pw}\frac{\partial T_{pw}}{\partial x} = \frac{FL}{U}\left(1 - T_{pw}\right) \tag{31}$$

respectively.

By using finite differences, Equations (29), (30) and (31) are reduced to

$$u_1^{n+1} = -\frac{2}{3}\frac{FL}{U}\Delta x + \frac{4}{3}u_1^n - \frac{1}{3}u_1^{n-1} \tag{32}$$

$${\rho_p}_1^{n+1} = \frac{2{\rho_p}_1^n - 0.5{\rho_p}_1^{n-1}}{1.5 - \frac{\frac{FL}{U}\Delta x}{{u_p}_1^{n+1}}} \tag{33}$$

$${T_p}_1^{n+1} = \frac{2{T_p}_1^n - 0.5{T_p}_1^{n-1} + \frac{FL}{U}\frac{\Delta x}{{u_p}_1^{n+1}}}{1.5 + \frac{FL}{U}\frac{\Delta x}{{u_p}_1^{n+1}}} \tag{34}$$

Heat transfer:

The heat transfer characteristic is expressed in terms of Nusselt number, given by

$$Nu^{\,n+1} = -\sqrt{Re}\left[\frac{\partial T}{\partial \eta}\right]_{\eta=0}^{n+1} = -\sqrt{Re}\left[\frac{T_{j+1}^{n+1} - (1-r_y^2)T_j^{n+1} - r_y^2\,T_{j-1}^{n+1}}{r_y(1+r_y)\Delta y}\right]_{j=2}$$

$$= -\sqrt{Re}\left[\frac{T_3^{n+1} - (1-r_y^2)T_2^{n+1} - r_y^2\,T_1^{n+1}}{r_y(1+r_y)\Delta y}\right] \tag{35}$$

Calculation of skin friction coefficient:

$$C_f = \frac{\tau_w}{0.5\rho U^2} = \frac{1}{0.5\rho U^2}\,\mu\frac{\partial u}{\partial y}\bigg]_{y=0} = \frac{2}{U^2\sqrt{Re}}\,\frac{\partial u}{\partial \eta}\bigg]_{\eta=0}$$

By using finite differences, the above equation reduces to

$$C_f^{n+1} = \frac{2}{U^2\sqrt{Re}}\left[\frac{u_{j+1}^{n+1} - (1-r_y^2)u_j^{n+1} - r_y^2\,u_{j-1}^{n+1}}{r_y(1+r_y)\Delta y}\right]_{j=2} = \frac{2}{U^2\sqrt{Re}}\left[\frac{u_3^{n+1} - (1-r_y^2)u_2^{n+1} - r_y^2\,u_1^{n+1}}{r_y(1+r_y)\Delta y}\right] \tag{36}$$

Discussion of results and conclusion:

Here in this problem, the basic features of the gas particulate thermal boundary layer flow over a semi-infinite flat plate have been studied by employing finite difference technique.

We choose the following values of the various parameters involved.

$$\rho = 0.9752 \;\; kg/m^3$$

$\rho_p = 800, 2403, 8010\ \ kg/m^3$ $\epsilon = 0.05, 0.1, 0.2$

$d = 50, 100\ \mu m$ $U = 60.96\ m/sec$

$\varphi = 0.001, 0.0003, 0.0001 L = 0.3048\ m$

$\alpha = 0.1$ $Ec = 0.1,\ Pr = 0.71, 1.0, 7.0$

$\mu = 1.5415 \times\ 10^{-5}\ kg/m\ sec$

To develop a computational algorithm with non-uniform-grid, finite difference expressions are introduced for the various terms in equations (8) to (14) to give rise to the equations (17) to (23).

At the wall $u_1 = 0$ and $y = y_{max}, u_{jmax} = U$. Equations (18) to (23) are repeated at $jmax - 2$ interior nodes forming a tri-diagonal system of equations that can be solved using the Thomas algorithm for $u_j^{n+1}, {u_p}_j^{n+1}$, ${v_p}_j^{n+1}$, T_j^{n+1}, ${T_p}_j^{n+1}$.

The continuity equation (8) is integrated across the boundary layer to give rise v_j^{n+1} using equation (17). The solution of the velocity and temperature distributions for both the phases and particle density in the boundary layer are obtained by solving equations (18) to (23) sequentially at each downstream location x^{n+1}.

As $\frac{\partial u}{\partial x}$ and other partial derivatives are represented by three level formulae (24) to (28), so two levels of data for u, v, u_p, v_p, T, T_p, ρ_p are required as initial conditions. The initial u, v, u_p, v_p, T, T_p, ρ_p profiles are prescribed from the standard solutions available for the boundary layer flow over a flat plate.

In the program of the initial profiles are obtained using the Lagrange interpolation and the values of u, v, u_p, v_p, T, T_p, ρ_p are produced at each downstream step along with the values of skin friction coefficient C_f, displacement thickness (DISP) and Nusselt number Nu.

To guarantee the best result from the program developed here, the program has been executed for several values of r_y, the grid growth ratio. At the end of downstream march, programme calculates the exact u velocity component u_{bx} , by interpolating UB, initial velocity profile for u and computes the root mean square(r. m. s.) error between u and u_{bx}. From some typical outputs of the program for fluid without SPM, we conclude that the result for r_y = 0.90 which gives least r. m. s. error between u and u_{bx} . Therefore the result for r_y = 0.90 is accepted and used for the physical interpretation of the result.

Similarly, the computational results for the flow of fluid with SPM are also obtained. It is observed that the result obtained for $r_y = 0.82$ is acceptable as r. m. s. error between u and u_{bx} is least.

To study the effect of various physical parameters on the velocity field, thermal boundary layer, shearing stress and coefficient of rate of heat transfer on the wall, the result obtained from numerical computation is depicted through Figures (1) to (13) and Tables (1) to (8). The values of Prandtl number P_r are taken as 0.71, 1.0 and 7.0 which physically correspond to air, electrolyte solution and water, respectively.

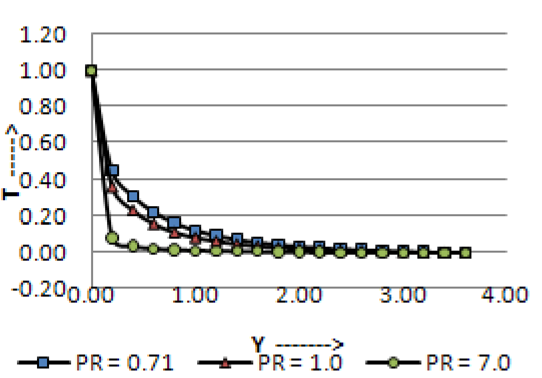

Fig. 1. Variation of temperature of carrier fluid T for different values of Pr

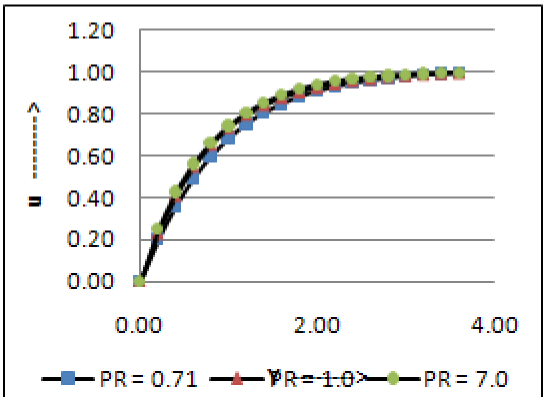

Fig. 2. Variation of velocity profile of carrier fluid u for different values of Pr

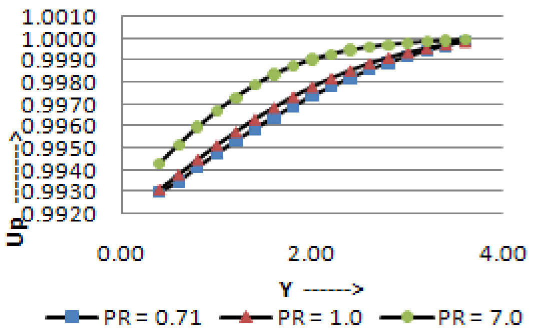

Fig . 3. Variation of particle velocity u_p for different values of *Pr*

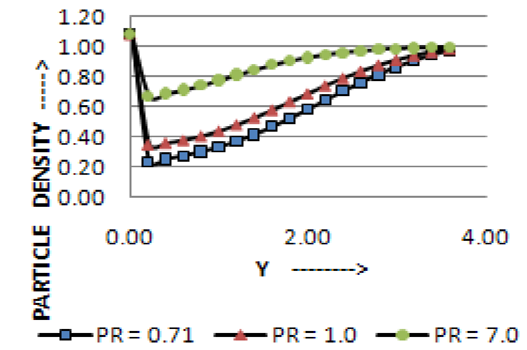

Fig . 4. Variation of particle density ρ_p for different values of *Pr*

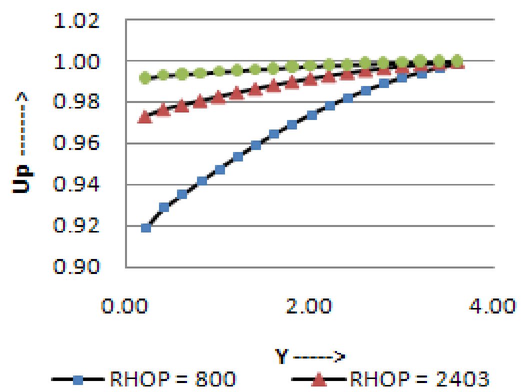

Fig . 5. Variation of particle velocity u_p for different values of material density of particle ρ_s

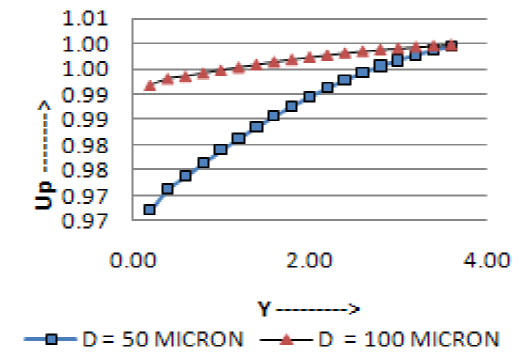

Fig . 6. Variation of particle velocity u_p for different size of particles *D*

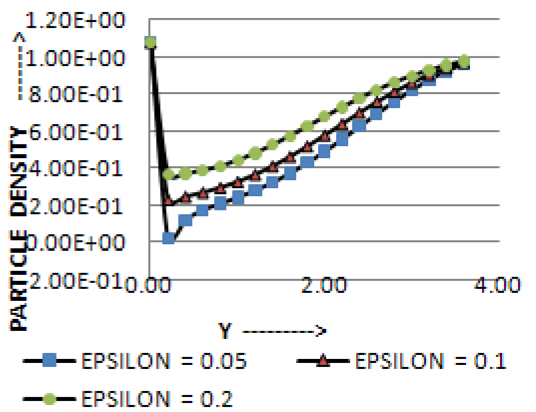

Fig . 7. Variation of particle density ρ_p for different values of ε

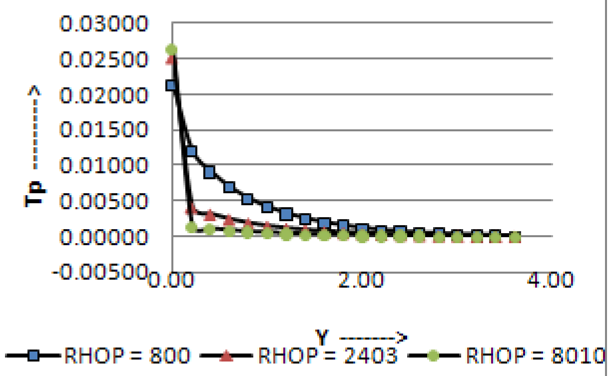

Fig . 8. Variation of particle temparature *Tp* for different values of material density of particle ρ_s

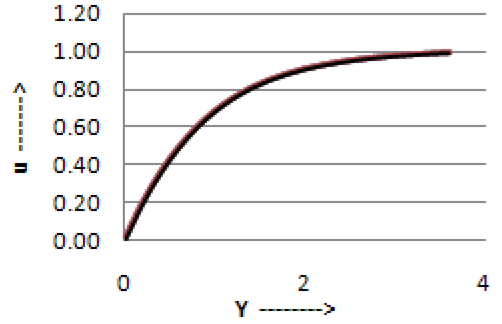

Fig. 9. Variation of velocity profile of carrier fluid u with y

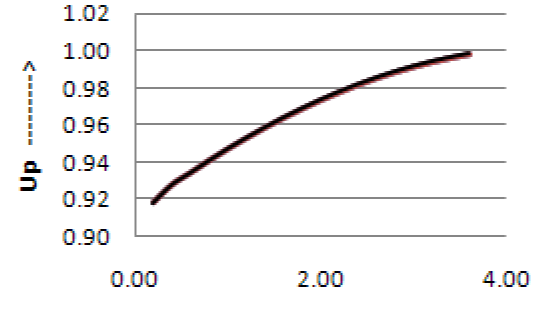

Fig. 10. Variation of particle velocity u_p with y

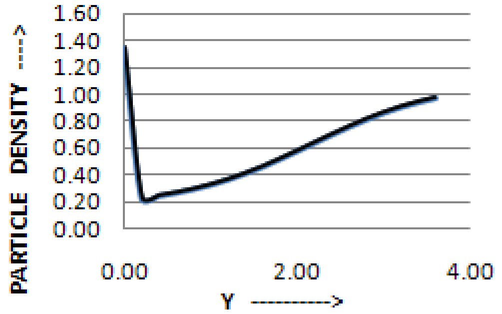

Fig. 11. Variation of particle density ρ_p with y

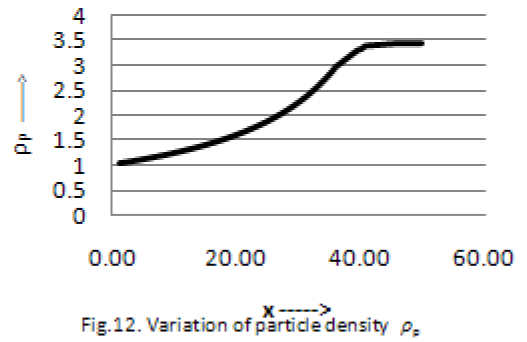

Fig. 12. Variation of particle density ρ_p towards downstream station

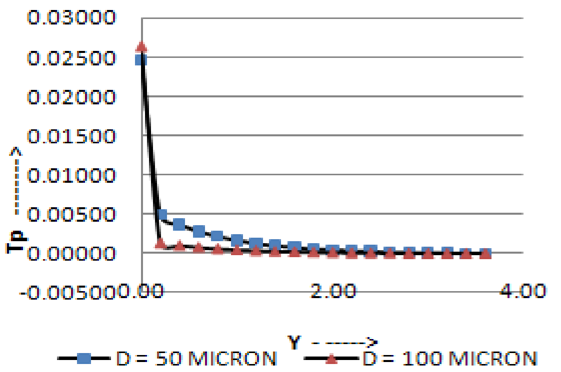

Fig. 13. Variation of particle temparature Tp for different size of particles D

It is observed from Figure1 that the thickness of thermal boundary layer is greater for air (P_r = 0.71) and more uniform temperature distribution across the thermal boundary layer as compared to water (P_r = 7.0) and electrolyte solution (P_r =1.0). Further the increase of P_r results in the decrease of temperature distribution. Physically, heat is diffused away from the heated surface more rapidly than for higher values of P_r, as smaller P_r indicates increase in thermal conductivity. Thus temperature falls more rapidly for water than that of air and electrolyte solution. The maximum temperature is observed in the vicinity of the plate and asymptotically approaches to zero in the free stream region. The same trend has been observed in case of particle temperature (T_p) from Table-1.

From Figures 2, 3 and 4, it is observed that the magnitudes of carrier fluid velocity $\boldsymbol{u}$, particle velocity $\boldsymbol{u_p}$, particle phase density $\boldsymbol{\rho_p}$ increases with the increase of P_r for a fixed value of volume fraction $\boldsymbol{\varphi}$ of the particles. Also, increase in magnitude of $\boldsymbol{u_p}$ and $\boldsymbol{\rho_p}$ are observed either (i) due to the presence of particles with high material density (Figure-5 and Table-2) or (ii) presence of coarser particles (Figure-6 and Table-3) or (iii) more diffusivity of the particles through the carrier fluid (Table 4 and Fig.7). Further as $\boldsymbol{T_p}$ decreases if particles of high material density are present but increases in case of more diffusivity of the particles (Figure-8 and Table-5). The magnitudes of $\boldsymbol{C_f}$ and Nu (Tables 6 and 7) increase with P_r but displacement thickness(Table-8) decreases with P_r. The magnitudes of skin friction coefficient C_f, displacement thickness and Nusselt number Nu (Tables 6, 8 and 7) increase for fluid flows with SPM of negligible Volume fraction as compared to those values for the flow of clear fluid. Figures 9, 10 and 11 displays the velocity profiles u, u_p and density profile ρ_p with respect to y. Figure-12 shows that the particle density on the plate goes on increasing and attains a finite value of 3.5 at a far downstream station and never attains an infinite value. Lastly, we observe from Figure-13 that the magnitude of particle temperature T_p decreases in the presence of the coarser particles.

Table 1. Variation of Particle temperature T_p for different P_r

Y	T_p for $P_r = 0.71$	T_p for $P_r = 1.0$	T_p for $P_r = 7.0$
0.00	2.63E-02	2.63E-02	2.63E-02
0.20	1.36E-03	9.80E-04	1.50E-04
0.40	1.03E-03	7.03E-04	2.85E-05
0.60	8.02E-04	5.27E-04	4.46E-06
0.80	6.23E-04	3.98E-04	7.15E-07
1.00	4.85E-04	3.03E-04	1.09E-06
1.20	3.79E-04	2.33E-04	1.68E-06
1.40	2.96E-04	1.79E-04	1.87E-06
1.60	2.31E-04	1.37E-04	1.74E-06
1.80	1.80E-04	1.06E-04	1.46E-06
2.00	1.40E-04	8.08E-05	1.15E-06
2.20	1.08E-04	6.14E-05	8.67E-07
2.40	8.23E-05	4.62E-05	6.34E-07
2.60	6.18E-05	3.42E-05	4.50E-07
2.80	4.53E-05	2.48E-05	3.11E-07
3.00	3.21E-05	1.73E-05	2.06E-07
3.20	2.14E-05	1.14E-05	1.29E-07
3.40	1.27E-05	6.70E-06	7.22E-08
3.60	5.70E-06	2.97E-06	3.05E-08

Table 2. Variation of Particle phase density ρ_p for various material density ρ_s

Y	ρ_s = 800	ρ_s = 2403	ρ_s = 8010
0.00	1.3462	1.1409	1.0834
0.20	0.2314	0.2317	0.2323
0.40	0.2477	0.2490	0.2499
0.60	0.2706	0.2715	0.2722
0.80	0.2974	0.2979	0.2985
1.00	0.3297	0.3302	0.3307
1.20	0.3683	0.3688	0.3693
1.40	0.4133	0.4140	0.4145
1.60	0.4644	0.4652	0.4657
1.80	0.5206	0.5215	0.5220
2.00	0.5804	0.5813	0.5818
2.20	0.6419	0.6428	0.6432
2.40	0.7030	0.7038	0.7041
2.60	0.7617	0.7623	0.7626
2.80	0.8162	0.8168	0.8170
3.00	0.8654	0.8658	0.8660
3.20	0.9084	0.9087	0.9088
3.40	0.9451	0.9452	0.9453
3.60	0.9754	0.9755	0.9755

Table 3. Variation of Particle phase density ρ_P for different size of particles *D*

Y	ρ_P for D= 50 micron	ρ_P for D= 100 micron
0.00	1.1585	1.0834
0.20	0.2315	0.2323
0.40	0.2488	0.2499
0.60	0.2713	0.2722
0.80	0.2978	0.2985
1.00	0.3301	0.3307
1.20	0.3687	0.3693
1.40	0.4139	0.4145
1.60	0.4651	0.4657
1.80	0.5214	0.5220
2.00	0.5812	0.5818
2.20	0.6427	0.6432
2.40	0.7037	0.7041
2.60	0.7623	0.7626
2.80	0.8167	0.8170
3.00	0.8657	0.8660
3.20	0.9087	0.9088
3.40	0.9452	0.9453
3.60	0.9755	0.9755

Table 4. Variation of Particle velocity u_p for various diffusion parameters ε

Y	u_p for $\varepsilon = 0.05$	u_p for $\varepsilon = 0.1$	u_p for $\varepsilon = 0.2$
0.00	0.9217	0.9217	0.9217
0.20	0.9964	0.9917	0.9918
0.40	0.9922	0.9930	0.9927
0.60	0.9931	0.9935	0.9935
0.80	0.9939	0.9941	0.9942
1.00	0.9945	0.9948	0.9949
1.20	0.9951	0.9953	0.9955
1.40	0.9956	0.9959	0.9961
1.60	0.9962	0.9964	0.9966
1.80	0.9967	0.9969	0.9971
2.00	0.9971	0.9974	0.9976
2.20	0.9976	0.9978	0.9980
2.40	0.9980	0.9982	0.9984
2.60	0.9984	0.9985	0.9987
2.80	0.9987	0.9989	0.9990
3.00	0.9990	0.9992	0.9993
3.20	0.9993	0.9994	0.9995
3.40	0.9996	0.9996	0.9997
3.60	0.9998	0.9998	0.9999

Table 5. Variation of Particle temperature T_p for various diffusion parameters ϵ

Y	T_p for $\epsilon = 0.05$	T_p for $\epsilon = 0.1$	T_p for $\epsilon = 0.2$
0.00	2.63E-02	2.63E-02	2.63E-02
0.20	8.50E-04	1.36E-03	1.64E-03
0.40	7.31E-04	1.03E-03	1.24E-03
0.60	6.39E-04	8.02E-04	9.54E-04
0.80	5.06E-04	6.23E-04	7.42E-04
1.00	3.95E-04	4.85E-04	5.81E-04
1.20	3.07E-04	3.79E-04	4.56E-04
1.40	2.38E-04	2.96E-04	3.59E-04
1.60	1.85E-04	2.31E-04	2.83E-04
1.80	1.43E-04	1.80E-04	2.22E-04

2.00	1.10E-04	1.40E-04	1.73E-04
2.20	8.40E-05	1.08E-04	1.34E-04
2.40	6.35E-05	8.23E-05	1.03E-04
2.60	4.73E-05	6.18E-05	7.78E-05
2.80	3.44E-05	4.53E-05	5.73E-05
3.00	2.42E-05	3.21E-05	4.07E-05
3.20	1.60E-05	2.14E-05	2.72E-05
3.40	9.46E-06	1.27E-05	1.63E-05
3.60	4.22E-06	5.70E-06	7.31E-06

Table 6. Variation of Skin friction coefficient C_f for different P_r

X	C_f for clear fluid	C_f for fluid with SPM, negligible φ	C_f for fluid with SPM with φ & Pr = 0.71	C_f for fluid with SPM with φ & Pr = 1.0	C_f for fluid with SPM with φ & Pr = 7.0
1.20	1.99E-03	1.95E-03	1.99E-03	2.07E-03	2.66E-03
1.60	2.10E-03	2.64E-03	3.48E-03	3.94E-03	4.62E-03
2.00	2.39E-03	2.05E-03	2.59E-03	2.86E-03	5.04E-03
2.40	2.59E-03	2.29E-04	3.16E-03	3.42E-03	3.74E-03
2.80	2.69E-03	9.23E-05	2.75E-03	3.14E-03	4.45E-03
3.20	2.75E-03	1.20E-04	3.01E-03	3.21E-03	4.48E-03
3.60	2.77E-03	1.27E-04	2.83E-03	3.24E-03	4.05E-03
4.00	2.80E-03	1.28E-04	2.95E-03	3.15E-03	4.38E-03
4.40	2.80E-03	1.28E-04	2.87E-03	3.25E-03	4.32E-03
4.80	2.80E-03	1.28E-04	2.92E-03	3.15E-03	4.19E-03
5.00	2.80E-03	1.28E-04	2.89E-03	3.19E-03	4.29E-03

Table 7. Variation of Nusselt number N_u for different P_r

X	N_u for clear fluid	N_u for fluid with SPM & negligible φ	N_u for fluid with SPM with φ & P_r = 0.71	N_u for fluid with SPM with φ & P_r = 1.0	N_u for fluid with SPM with φ & P_r = 7.0
1.20	2.63E+03	6.29E+02	8.52E+01	3.16E+02	5.12E+03
1.60	3.31E+03	4.72E+03	1.20E+04	2.08E+04	1.51E+05
2.00	3.31E+03	5.10E+03	1.09E+04	1.94E+04	1.34E+05
2.40	3.31E+03	2.06E+03	1.17E+04	2.01E+04	1.32E+05
2.80	3.31E+03	3.43E+03	1.11E+04	1.98E+04	1.33E+05
3.20	3.31E+03	3.44E+03	1.15E+04	1.98E+04	1.32E+05
3.60	3.31E+03	3.44E+03	1.13E+04	2.00E+04	1.32E+05
4.00	3.31E+03	3.44E+03	1.14E+04	1.97E+04	1.32E+05
4.40	3.31E+03	3.44E+03	1.13E+04	1.99E+04	1.32E+05
4.80	3.31E+03	3.44E+03	1.14E+04	1.98E+04	1.32E+05
5.00	3.31E+03	3.44E+03	1.13E+04	1.98E+04	1.32E+05

Table 8. Variation of Displacement thickness (DISP) for different P_r

X	DISP for clear fluid	DISP for fluid with SPM negligible φ	DISP for fluid with SPM with φ & P_r = 0.71	DISP for fluid with SPM with φ & P_r = 1.0	DISP for fluid with SPM with φ & P_r = 7.0
1.20	5.37E-03	4.76E-03	4.24E-03	3.89E-03	2.87E-03
1.60	5.05E-03	3.82E-03	3.06E-03	2.77E-03	2.32E-03
2.00	4.66E-03	5.09E-03	3.68E-03	3.29E-03	2.11E-03
2.40	4.45E-03	7.75E-03	3.27E-03	3.04E-03	2.49E-03
2.80	4.35E-03	7.84E-03	3.55E-03	3.13E-03	2.31E-03
3.20	4.29E-03	7.82E-03	3.38E-03	3.14E-03	2.27E-03
3.60	4.27E-03	7.81E-03	3.49E-03	3.09E-03	2.41E-03
4.00	4.25E-03	7.81E-03	3.42E-03	3.16E-03	2.32E-03
4.40	4.24E-03	7.81E-03	3.46E-03	3.09E-03	2.32E-03
4.80	4.24E-03	7.81E-03	3.44E-03	3.15E-03	2.36E-03
5.00	4.24E-03	7.81E-03	3.46E-03	3.12E-03	2.33E-03

Nomenclature

$\vec{q}(u, v)$	Velocity components for the fluid phase in x- and y- directions respectively
$\overrightarrow{q_p}(u_p, v_p)$	Velocity components for the particle phase in x-and y- directions respectively
$\overrightarrow{q_m}(u_m, v_m)$ $(T,\ T_p)$	Velocity components for the mixture in x-and y- directions respectively Temperatures of fluid and particle phase
(T_w, T_∞)	Temperature at the wall and free-stream respectively
(ν, ν_p)	Kinematics coefficient of viscosity of fluid and particle phase respectively
(ρ, ρ_p)	Density of fluid and particle phase respectively
(ρ_s, ρ_m)	Material density of particle(RHOS) and mixture respectively
P_r	Prandtl number
E_c	Eckret number
N_u	Nusselt number
C_f	Skin friction coefficient
φ D	Volume fraction of SPM Diameter of the particle
U	Free stream velocity
μ	Coefficient of viscosity of fluid
δ	Boundary layer thickness
τ_T	Thermal equilibrium time
T_0	Temperature of the plate at $\eta = 0$
ρ_{p0}	Density of particle phase in free stream
a	Thermal diffusivity
κ	Thermal conductivity
α	Concentration parameter
ε	Diffusion parameter(EPSILON)
F	Friction parameter between the fluid and the particle $\left(F = 18\mu/\rho_p d^2\right)$
J_{max}	Maximum number of Grid points along Y – axis
L $W(x, y)$ r_y u_{pw} ρ_{pw} T_{pw}	Reference length Dummy variable Grid growth ratio Particle velocity on the plate Particle density distribution on the plate Temperature of particle phase on the plate
D_p	Binary diffusion coefficient

References:

[1] Soo S L. Laminar and separated flow of a particulate suspension, Astronautica Acta, 11(1965), 422-431.

[2] Singleton R E. The compressible gas – solid particles flow over a semi – infinite flat plate, ZAMP, 16 (1965), 421 – 449.

[3] Otterman B. Particle migrations in laminar mixing of a suspension with a clear fluid, ZAMP, 20 (1969), 730-749.

[4] Jain A C, Ghosh A. Gas particulate laminar boundary layer on a flat plate, Z.F.W. , 3 (1979), 29-37.

[5] Prabha S, Jain A C. Laminar boundary layer of gas particulate flow on a flat plate, Proceedings of Indian Acad. Science, 88A-III(5), (1979), 377-385.

[6] Ahamadi G A. Continuum theory for two phase media, Acta Mech. 44 (1982), 299 – 317.

[7] Chamkha A J. Hydromagnetic two-phase flow in a channel, International Journal of Engineering Science, 33(3), (1995), 437 – 446.

[8] Chamkha A J. Solutions for fluid particle-flow and heat transfer in a porous channel, International Journal of Engineering Science, 34(2), (1996), 1423 – 1439.

[9] Panda T C, Mishra S K and Panda K C. Laminar diffusion of suspended particulate matter using a two phase flow model, Int. J. for Numerical Methods in Fluids, 40 (2002), 841-853.

[10] Panda T C, Mishra S K and Panda K C. Volume fraction and diffusion analysis in SPM modeling in an inertial frame of reference, Acta Ciencia Indica, 27 M(4),(2001), 515-525.

[11] Panda T C, Mishra S K and Dash D K. Modeling dispersion of SPM in free convection flows in the vicinity of heated horizontal flat plate, Impact J. Sc. Tech, 1(1) (2007), 37-60.

[12] Marble F E. Dynamics of a gas combining small solid particles, Fifth AGARD combustion and propulsion colloquium, (Pergamon Press) Oxford, England, 1963, pp. 175-215.

[13] Soo S L. Fluid dynamics of Multiphase systems, Blasisdell publishing company. London, 1968, 248-256.

[14] Raviart P A, Sainsulies L. Mathematical and Numerical modeling of two phase flows. In Glowiniki; editor: New Work, Nova Science Publisher, 1991, 119 – 123.

[15] Mishra S K, Tripathy P K. Approximate solution of two phase thermal boundary layer flow, Reflections des ERA, July 2011, (In Press).

[16] Mishra S K, Tripathy P K. Mathematical and Numerical modeling of two phase flow and heat transfer using non-uniform grid, Far East Journal of Applied Mathematics, July 2011, (In Press).

[17] Misra A, Mishra S K and Prakash J. Modelling of electrification of suspended particulate matter(SPM) in a two phase boundary layer flow and heat transfer over a semi-infinite flat plate, ICHMT-02407, Int. Commun. Heat Mass Transf., July 2011.

[18] Soo S L, Boundary layer motion of a gas solid suspension, University of Illinois, Project squid Report, ILL-3p, 1961.

[19] Chiu H H. Boundary layer flow with suspended particles, Princeton University, Report 620, 1962.